Journal of Low Temperature Physics, Vol. 93, Nos. 1/2, 1993

Thermodynamic Stability of the Superconducting Phase Diagram of UPt_3

N. H. van Dijk, A. de Visser, and J. J. M. Franse

Van der Waals-Zeeman Laboratory, University of Amsterdam, Valckenierstraat 65, 1018 XE Amsterdam, The Netherlands

and

L. Taillefer

Department of Physics, McGill University, H3A 2T8 Montreal, Canada

(Received April 6, 1993)

The superconducting phase diagram of UPt_3, *as determined by accurate dilatometry as function of temperature and magnetic field* ($B \parallel c$ *and* $B \perp c$), *exhibits three superconducting phases which meet in a tetracritical point. We show that the measured phase diagrams are thermodynamically stable and that all four phase lines are of second order. Via Ehrenfest relations the pressure dependence of the various phases has been determined. The so-called* C *phase is the most stable phase under uniaxial pressure along the c-axis* ($p_c > 2.5$ *kbar*). *The resulting phase diagram in the* p_c-T *plane yields stringent constraints on the fourth order coupling constants in the Ginzburg-Landau scenario of a vector superconducting order parameter coupled to a symmetry breaking field.*

1. INTRODUCTION

The heavy fermion superconductor UPt_3 is one of the strongest candidates for unconventional superconductivity. Specific-heat measurements[1–3] on poly and single-crystalline samples prepared in different ways showed the existence of a double superconducting transition. The second transition is located approximately 60 mK below the first transition within the superconducting state. Measurements of the specific heat,[4] the sound velocity[5,6] and the thermal expansion[7] in a magnetic field revealed a complex superconducting phase diagram with three superconducting phases which meet at a tetracritical point (TP).

0022-2291/93/1000-0101$07.00/0

The exotic superconducting phase diagram of UPt_3 is described to a large extent by phenomenological Ginzburg-Landau models in which the free energy is expanded in terms of an unconventional superconducting vector order parameter.[8–13] In the most plausible model the superconducting vector order parameter couples to a symmetry breaking field (SBF), which lifts the degeneracy of the order parameter. As a result various superconducting phases are found in a way similar to superfluid ^{3}He. The symmetry breaking field possibly originates in the antiferromagnetic state with an extremely small ordered moment ($|\boldsymbol{\mu}| = 0.02\,\mu_B/U$-atom) that is detected by neutron diffraction[14] below $T_N = 5$ K. The available Ginzburg-Landau scenarios are, however, still subject to lively debates, as they are inadequate at several points, in particular with respect to the topology of the phase diagram.[15]

Another important aspect of the proposed superconducting phase diagrams for UPt_3 is the thermodynamic stability. This issue was recently investigated by Yip and coworkers,[16] by studying the thermodynamics of bicritical and tetracritical points, where at least two or three second order phase transition lines intersect. The authors showed that the thermodynamic stability of a tetracritical point places severe restrictions on the topology of the phase diagram. This makes a stability analysis a strong tool for the interpretation of the proposed phase diagrams.

Recently, we have reported detailed thermal-expansion and magnetostriction measurements[17] of the superconducting phases of single-crystalline UPt_3 for magnetic fields directed along the a- and b-axis in the hexagonal plane ($a \perp b$). In this paper complementary results of the thermal expansion and magnetostriction for a field along the hexagonal c-axis are presented. The thermodynamic stability of the resulting superconducting phase diagrams ($B \perp c$ and $B \parallel c$) is investigated in connection with the presence of a tetracritical point. Using Ehrenfest relations the uniaxial pressure dependence of the superconducting phases has been determined.[17] We also report on the constraints on the Ginzburg-Landau model parameters inferred from the phase diagram under pressure.

2. EXPERIMENTAL RESULTS

Dilatometry experiments were performed on a single-crystalline UPt_3 sample (dimensions $a \times b \times c = 3 \times 1 \times 2\,\text{mm}^3$). The tiny sample was cut from a poly-crystalline rod with large grains prepared under ultra high vacuum conditions. The coefficient of linear thermal expansion, $\alpha(T) = L^{-1}dL/dT$, and the linear magnetostriction, $\lambda(B) = (L(B) - L(0))/L(0)$, were measured using a sensitive parallel-plate capacitance dilatometer. Experimental details can be found in Ref. 17. Measurements for a dilatation

(contraction) along the c-axis have been performed for $B \| a$ and $B \| b$ (see Ref. 17), and for $B \| c$. Experiments for a dilatation (contraction) along the a-axis have only been performed in zero field so far.

The coefficients of linear thermal expansion along the a- and c-axis, α_a and α_c, in zero field, are shown in Fig. 1. The thermal expansion is strongly anisotropic. Along the c-axis two clear steps of opposite sign, located at $T_c^+ = 0.493(2)$ K and $T_c^- = 0.438(2)$ K, mark the double superconducting transition. Along the a-axis a kink is observed at T_c^+, while a small step is found at T_c^-. The volume expansion is given by $\alpha_v = 2\alpha_a + \alpha_c$ and shows two steps of identical sign. The step at T_c^+ is much larger then the step at T_c^-.

In Fig. 2 we show a few exemplary thermal-expansion curves taken in a constant applied field ($B \| c$). Both T_c^+ and T_c^- are suppressed with field,

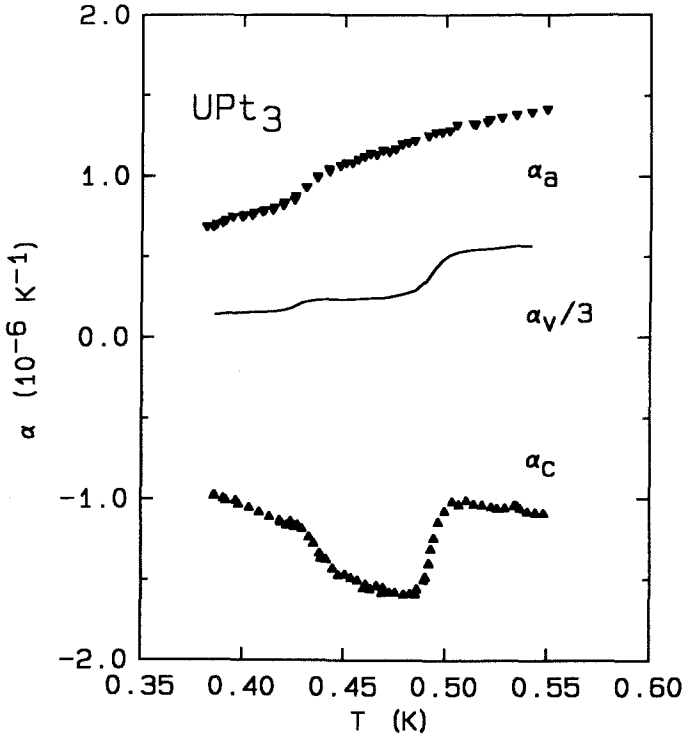

Fig. 1. The coefficients of linear thermal expansion of UPt_3 along the a-axis and the c-axis in the vicinity of the double superconducting transition. The solid line represents one third of the linear coefficient of volume thermal expansion $\alpha_V/3 = (2\alpha_a + \alpha_c)/3$.

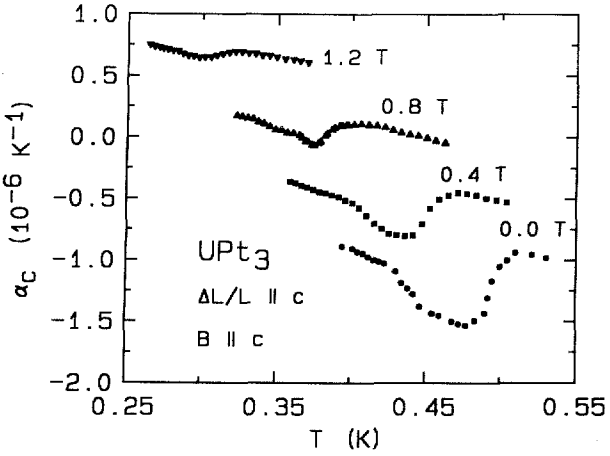

Fig. 2. The coefficient of linear thermal expansion for $\Delta L/L \parallel c$ for some characteristic fields ($B \parallel c$). The curves in field are shifted along the vertical axis for sake of clarity.

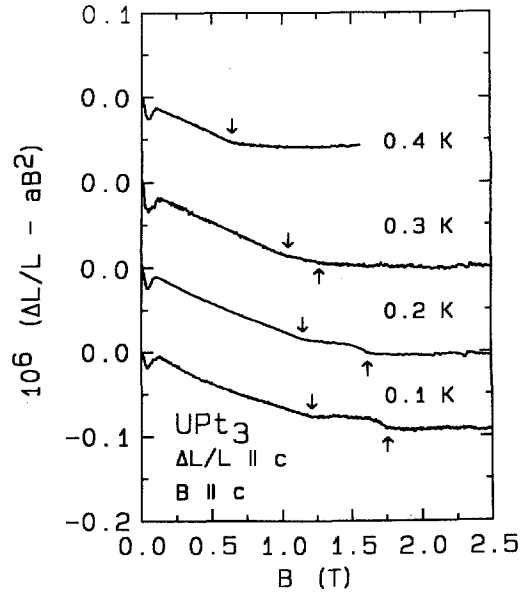

Fig. 3. Magnetostriction of UPt_3 for $\Delta L/L \parallel c$ and $B \parallel c$ for some characteristic temperatures. The quadratic background of the normal state is subtracted for sake of clarity. The anomalies at the superconducting transitions are indicated by arrows. The low field anomaly at $B = 0.1$ T is not connected to superconductivity.

but T_c^+ is suppressed more rapidly than T_c^-, so that the transitions merge for a critical field B_{cr}. For $B > B_{cr}$ only a single transition remains.

A few typical magnetostriction curves, $\lambda(B)$, for a field and dilatation direction along the c-axis are shown in Fig. 3. Pronounced anomalies appear after subtracting a term quadratic in field, representative for the magnetostriction of the normal state. At low temperatures the kink signals a transition within the superconducting state, while the upper anomaly marks the transition to the normal state. For $T > T_{cr}$ only a single transition, i.e. to the normal state, remains. An additional anomaly is observed at $B = 0.1\ T$ for all field orientations ($B \parallel c$ and $B \perp c$). This anomaly is also found in the normal phase and is, therefore, not related to superconductivity. The data reported in Ref. 17, for a field in the hexagonal plane, suggested that the anomaly is possibly caused by a reorientation of the antiferromagnetic domains, which are formed below $T_N = 5$ K (the zero-field antiferromagnetic moment points along the b-axis). The observation of a similar anomaly for $B \parallel c$ does not support this suggestion, unless one assumes that the magneto-crystalline anisotropy is small enough for the magnetic moments to align along the hexagonal axis in a field of 0.1 T. Neutron-diffraction measurements in a magnetic field are necessary to elucidate this point.

3. THE PHASE DIAGRAMS FOR $B \perp c$ AND $B \parallel c$

Locating the anomalies at the superconducting phase boundaries, detected by the thermal expansion and the magnetostriction technique, in the B-T plane the superconducting phase diagrams of Fig. 4 result. The phase diagrams show three superconducting phases (labeled A, B and C). For both field orientations the three superconducting phases and the normal state (N) meet at a tetracritical point. The TP is located at $T_{cr} = 0.389(3)$ K and $B_{cr} = 0.443(5)\ T$ for $B \perp c$ and at $T_{cr} = 0.351(3)$ K and $B_{cr} = 0.948(5)\ T$ for $B \parallel c$. No significant anisotropy was observed for fields in the basal plane ($B \parallel a$ and $B \parallel b$). Notice that the phases labeled C for $B \perp c$ and $B \parallel c$ are not necessarily identical.

A blow up of the phase diagrams in the vicinity of the TP is shown in Fig. 5. The solid lines are obtained by a fitting procedure and indicate the slopes of the phase lines close to the TP. The dashed line marks the location of the low-field anomaly at $B = 0.1\ T$ observed in the magnetostriction. For $B \perp c$ the low-field anomaly coincides with a change of slope of the AB phase line, suggesting a coupling of superconductivity and antiferromagnetism for this particular field direction.

In the proposed Ginzburg-Landau scenario with a symmetry breaking field the three superconducting phases have different order parameters.

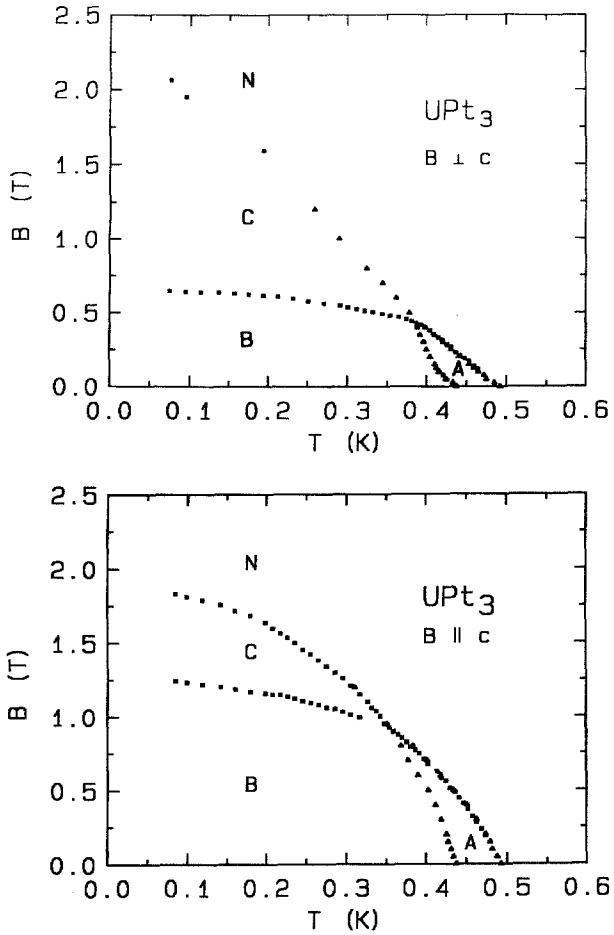

Fig. 4. The superconducting phase diagram of UPt_3 for $B \perp c$ and $B \| c$, constructed from the anomalies detected in the thermal expansion (▲) and the magnetostriction (■).

Symmetry arguments lead to the choice of the E_{1g} basis vectors for the order parameter. The hybrid gap function is given by $\psi(\mathbf{k}) = \eta_x k_x k_z + \eta_y k_y k_z$, where the complex vector $\boldsymbol{\eta} = (\eta_x, \eta_y)$ determines the order parameter. The A, B and C phase then correspond to the $(1, 0)$, the $(1, i)$ and the $(0, 1)$ phase, respectively.

4. THERMODYNAMIC STABILITY OF THE *B-T* PHASE DIAGRAM

In this section we investigate the thermodynamic stability of the superconducting phase diagrams of UPt_3 as reported in Fig. 4. We first comment

on the order of the phase lines. Specific-heat measurements[4,7] yield steps at the *NA*, *AB* and *NC* phase boundaries and no latent heat. This strongly suggests that these transitions are of second order, which is supported by the absence of hysteresis. Concerning the *BC* transition, the absence of hysteresis in the magnetostriction and the small magnetocaloric effect[18] also suggests second order. In general for a type II superconductor the transition at the upper critical field (B_{c2}) is of second order.

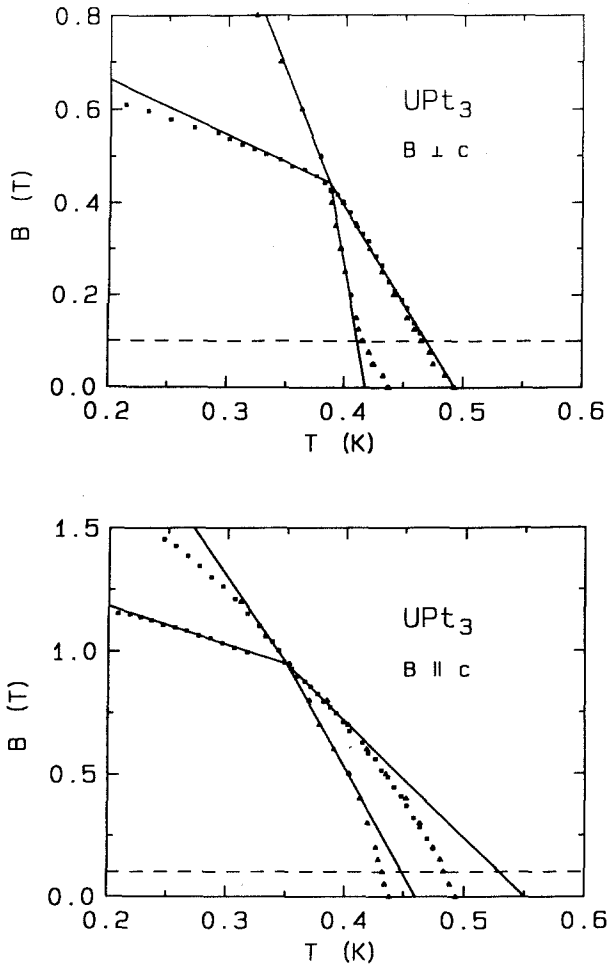

Fig. 5. The phase diagram of UPt_3 in the vicinity of the *TP*. The solid lines represent the fitted slopes of the phase lines near the *TP*. The dashed line indicates the location of the low field anomaly at $B = 0.1\ T$ in the magnetostriction.

The thermodynamic stability of a phase diagram with a tetracritical point, where at least three second order phase transition lines meet, was recently investigated by Yip and coworkers[16] by analysing the Gibbs free energy $G(T, B)$ near the critical point. The continuity of G, the entropy S and the magnetisation M at the second order phase lines, in combination with the requirement that the steps in c/T at all the phase lines are positive (when the temperature is lowered), leads to strict conditions for the slopes of all the phase lines and the order of the emerging fourth phase line. The stability criterion is formulated as a relation between the slopes of the phase lines and the steps in the specific heat at the phase transitions. Below we apply this criterion to the phase diagrams of UPt_3.

We introduce p_1, p_2, p_3 and p_4 for the slopes dB/dT of the phase lines NA, NC, AB and BC in the vicinity of the TP, respectively, and r_1^2, r_3^2 and r_4^2 as the ratios of the stepsizes in the specific heat $\Delta c_{NA}/\Delta c_{NC}$, $\Delta c_{AB}/\Delta c_{NC}$ and $\Delta c_{BC}/\Delta c_{NC}$ near the TP, respectively. The stability criterion for a TP with three second order phase lines NA, NC and AB is given by (conform Ref. 16)

$$(1-p_{41})\,r_1^2+p_{13}(1-p_{13}\,p_{41})\,r_3^2=p_{12}(1-p_{12}\,p_{41})+E^{1/2} \tag{1}$$

where

$$E=(1-p_{12})^2\,r_1^2+(p_{13}-p_{12})^2\,r_3^2-(1-p_{13})^2\,r_1^2r_3^2 \tag{2}$$

and $p_{ij}=p_i/p_j$. The sum of the steps in the specific heat just below the TP ($B<B_{cr}$) is equal to the sum of the steps just above the TP ($B>B_{cr}$) and therefore the ratio r_4^2 is directly related to the other ratios by $r_1^2+r_3^2=1+r_4^2$.

Using the experimental values for p_1, p_2, p_3 and p_4 as listed in Table I, we have plotted r_3^2 as function of r_1^2 (eq. 1 and 2) for $B\perp c$ in Fig. 6. A similar curve is found for $B\parallel c$ (not shown). Stable solutions can only appear for $r_4^2>0$ and thus for $r_1^2+r_3^2>1$, i.e. in the region above the dashed line of Fig. 6. Consequently, no stable solutions are found in the

TABLE I

Experimental Values of the Slopes of the Phase Lines near the TP for $B\perp c$ and $B\parallel c$ (see Fig. 5)

	$p_1\,(T/K)$	$p_2\,(T/K)$	$p_3\,(T/K)$	$p_4\,(T/K)$
$B\perp c$	−4.15	−6.35	−14.2	−1.19
$B\parallel c$	−4.76	−6.34	−8.70	−1.57

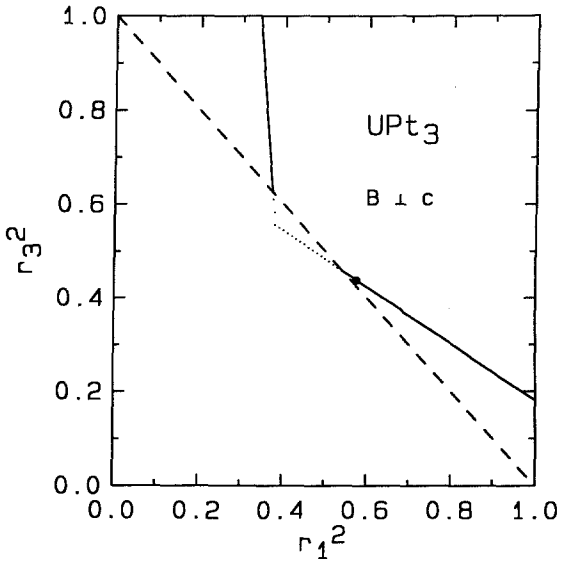

Fig. 6. Stability conditions of the Phase Diagram of UPt_3 for $B \perp c$. The solid lines indicate the stable solutions according to eq. 1 and 2. The area above the dashed line corresponds to the stability condition $r_4^2 \geq 0$. The solid dot (●) close to the dashed line is the relevant solution ($E = 0$) for the measured phase diagram ($r_1^2 = 0.58$, $r_3^2 = 0.43$ and $r_4^2 = 0.01$).

range $0.37 < r_1^2 < 0.54$ for $B \perp c$ and in the range $0.40 < r_1^2 < 0.46$ for $B \parallel c$. Experimental values for r_1^2 and r_3^2 have been determined from the specific-heat data in an applied magnetic field.[4,7] The step sizes at the *NA*, *AB* and *NC* transition as function of field for $B \perp c$ and $B \parallel c$ are shown in Fig. 7. The resulting values for r_1^2 and r_3^2 are listed in Table II. Note that the

TABLE II

Ratios of the Stepsizes in the Specific Heat near the *TP*, $r_1^2 = \Delta c_{NA}/\Delta c_{NC}$ and $r_3^2 = \Delta c_{AB}/\Delta c_{NC}$, for $B \perp c$ and $B \parallel c$, as Calculated Using the Stability Criterion with $E = 0$ and as Determined by Experiment[4,7]

	Calculation		Experiment	
	r_1^2	r_3^2	r_1^2	r_3^2
$B \perp c$	0.58(4)	0.43(4)	0.65(8)	0.35(8)
$B \parallel c$	0.52(4)	0.49(4)	0.47(5)	0.53(5)

experimental sum $r_1^2 + r_3^2$ is approximately 1 for $B \perp c$ and $B \| c$, indicating that the ratio r_4^2 is much smaller than the other ratios. The experimental values for r_1^2 amount to 0.65 for $B \perp c$ and to 0.47 for $B \| c$ and fall in the stability range. If furthermore BC is a second order transition then $E = 0$. This condition gives two stable solutions. The corresponding values for r_1^2 and r_3^2 (for the solution closest to the dashed line, i.e. for small r_4^2) are also listed in Table II. In Fig. 6 this solution is indicated by a large dot.

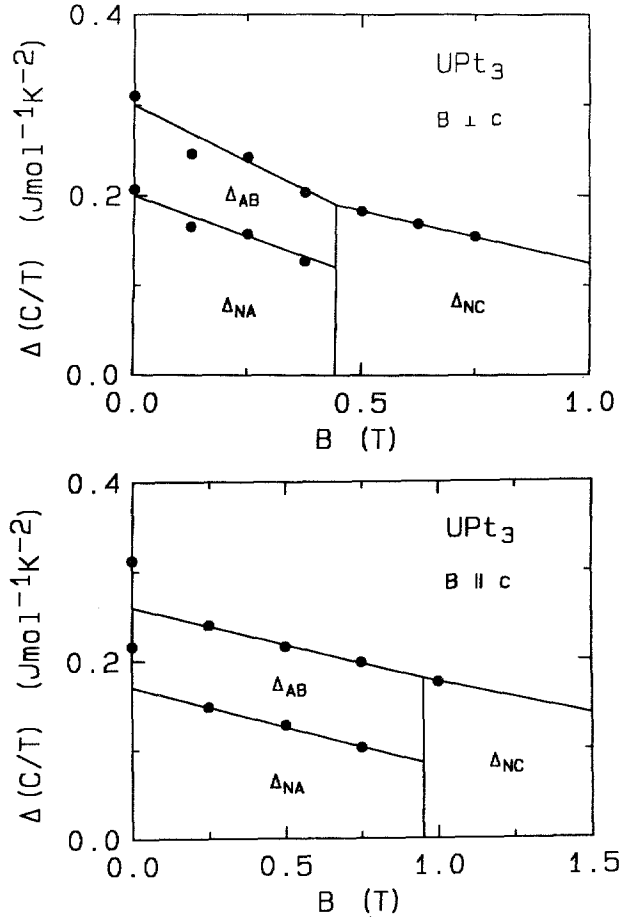

Fig. 7. Stepsizes in c/T at the superconducting transitions as function of field for $B \perp c$ and $B \| c$ (after Hasselbach *et al.*[4,7]). The solid lines are fits to the datapoints in the vicinity of the critical field B_{cr}. The critical field is indicated by the vertical line. Note that the difference between the solid lines below B_{cr} corresponds to the stepsize in c/T at the AB transition (Δ_{AB}).

Comparing the calculated and experimental values of r_1^2 and r_3^2 we conclude that the BC phase line can be of second order with $r_4^2 = 0.01$ for $B \perp c$ and $B \| c$. Hence $\Delta c_{BC} \simeq 1$ mJ/molK for both field orientations.

In summary, the stability analysis shows that for both field directions ($B \perp c$ and $B \| c$) the phase diagram with a tetracritical point is thermodynamically stable. Because hysteresis effects are absent (within the experimental accuracy) it is most likely that all four phase lines are of second order ($E = 0$), although a weakly first order BC transition can not be excluded (in that case $E < 5 \times 10^{-3}$).

Recently, Adenwalla and coworkers[19] have analysed the phase diagram of UPt_3 constructed from ultra sound measurements and concluded that the phase diagram can only be stable if the BC phase line is of first order. However, their analysis of the specific-heat data yields $r_1^2 = 1$ and $r_3^2 = 0$, which is inconsistent with experiments (see Fig. 7).

5. STABILITY OF THE PHASE DIAGRAM UNDER PRESSURE

In order to determine the uniaxial pressure dependence of the superconducting phase lines we apply the Ehrenfest relations:

$$\left(\frac{\partial T}{\partial p_i}\right)_{Bp'} = \frac{V_m \Delta \alpha_i}{\Delta (c/T)} \tag{3}$$

where $p_i (i = a, b, c)$ refers to a uniaxial pressure along the different crystallographic axes. The hydrostatic pressure dependence can be calculated according to $dT_c/dp = 2dT_c/dp_a + dT_c/dp_c$.

Using the thermal-expansion data of Fig. 1 and the specific-heat data of Hasselbach and coworkers[4,7] we calculate the following values for the uniaxial pressure dependences of T_c^+ and T_c^-: $dT_c^+/dp_a = 0.0$ mK/kbar, $dT_c^-/dp_a = -4.9$ mK/kbar, $dT_c^+/dp_c = -13.5$ mK/kbar and $dT_c^-/dp_c = 8.8$ mK/kbar. The uniaxial pressure dependence of T_c is highly anisotropic. For $p \| c$ the splitting $\Delta T_c = T_c^+ - T_c^-$ decreases at a rate $d\Delta T_c/dp_c = -22.3$ mK/kbar, while for $p \perp c$ ΔT_c increases: $d\Delta T_c/dp_a = 4.9$ mK/kbar. Assuming a linear pressure relation we find that for $p \| c$ the A phase vanishes at $T_{cr} = 0.460$ K and $p_{cr} = 2.5$ kbar. For hydrostatic pressure the A phase vanishes at $T_{cr} = 0.434$ K and $p_{cr} = 4.4$ kbar. In Fig. 8 we compare our calculated uniaxial pressure dependence of T_c^+ and T_c^- with the values evaluated by Jin and coworkers[20] from specific-heat experiments under uniaxial pressure. The agreement is satisfactory. In Table I we present an overview of experimental values for the uniaxial and hydrostatic pressure dependences of T_c^+ and T_c^- obtained by different techniques on various samples.[21–26] The values for dT_c^+/dp range from -14 to -26 mK/kbar,

while the values for dT_c^-/dp range from -5 to 0, indicating a considerable spread. The values calculated from the Ehrenfest relations tend to be the lowest.

Next we discuss the phase diagram in the uniaxial pressure-temperature plane ($p \| c$) and its thermodynamic stability. The specific-heat measurements under pressure[20] indicate that for $p \| c$ at least three phase lines meet in a critical point (T_{cr}, p_{cr}). A bicritical point of three second order phase lines in the p_c-T plane is only stable if $\Delta c_{NA}(p_{cr}) = 0$ or $\Delta c_{AB}(p_{cr}) = 0$ or when the three phase lines are tangential[16,19] at $p_c = p_{cr}$. The specific-heat measurements show that neither Δc_{NA} nor Δc_{AB} vanishes at p_{cr}. The third condition can be related to the pressure dependence of $\Delta T_c = (p_c - p_{cr})^\alpha$. For $\alpha = 1$ the phase lines in the p_c-T plane are straight lines and the condition is not fulfilled. Stability of a bicritical point is found for $\alpha > 1$. The experimental value for α amounts to 2.6 ± 1.9 (for hydrostatic pressure[27]). The uncertainty in α is however far too large to proof the existence of a bicritical point.

Another possibility is that a fourth phase line emerges from (T_{cr}, p_{cr}) so that a *TP* is also found in the p_c-T plane, as indicated in Fig. 8. The missing phase line must have a weak temperature dependence as it has not been detected in specific-heat measurements under pressure.[20,25] However, its existence can be inferred from the uniaxial pressure dependence of the B-T phase diagram ($p \| c$) as calculated with the Ehrenfest relations.[17] The uniaxial pressure dependence of the BC phaseline in the vicinity of the *TP* is large (we calculate $dT/dp_c \simeq -170$ mK/kbar for $B \perp c$) as the step in the specific heat is very small. The uniaxial pressure dependence of the *NC* phase line is weak (we calculate $dT/dp_c = -0.5$ mK/kbar for $B \perp c$ in accordance with resistivity measurements under pressure[22] and $dT/dp_c = -3.0$ mK/kbar for $B \| c$). Therefore, also the B phase is suppressed for $p \| c$ at moderate pressures (2-3 kbar) (for $B \| c$ and $B \perp c$) and the C phase is the most stable phase under pressure. Our analysis[17] shows that the missing fourth phase line is the *BC* phase line, hence a tetracritical point is also found in the p_c-T plane.

In the Ginzburg-Landau approach the double superconducting transition of UPt_3 is generally attributed to the lifting of the degeneracy of a vector order parameter $\boldsymbol{\eta} = (\eta_1, \eta_2)$ by a symmetry breaking field δ, in both one and two-dimensional representations.[9–11,13]. The free energy for a hexagonal system in a two-dimensional representation with a *SBF* is given by:[9–11]

$$F = \alpha |\boldsymbol{\eta}|^2 + \frac{\beta_1}{2} |\boldsymbol{\eta}|^4 + \frac{\beta_2}{2} |\boldsymbol{\eta}^2|^2 - \delta(|\eta_1|^2 - |\eta_2|^2) \tag{4}$$

where $\alpha = \alpha_o(T - T_{co})$. The suppression of the splitting of T_c can be described by a vanishing of the *SBF*. In most models the weak

antiferromagnetic moment is thought to act as the *SBF*, in which case $\Delta T_c \propto \delta \propto |\boldsymbol{\mu}|^2$. Recently, support for this idea has been obtained from hydrostatic pressure experiments, which showed that both $|\boldsymbol{\mu}|^2$ (determined by neutron diffraction[27]) and ΔT_c (measured by specific heat[25]), are suppressed linearly with pressure and both vanish at approximately the same critical pressure ~ 4 kbar.

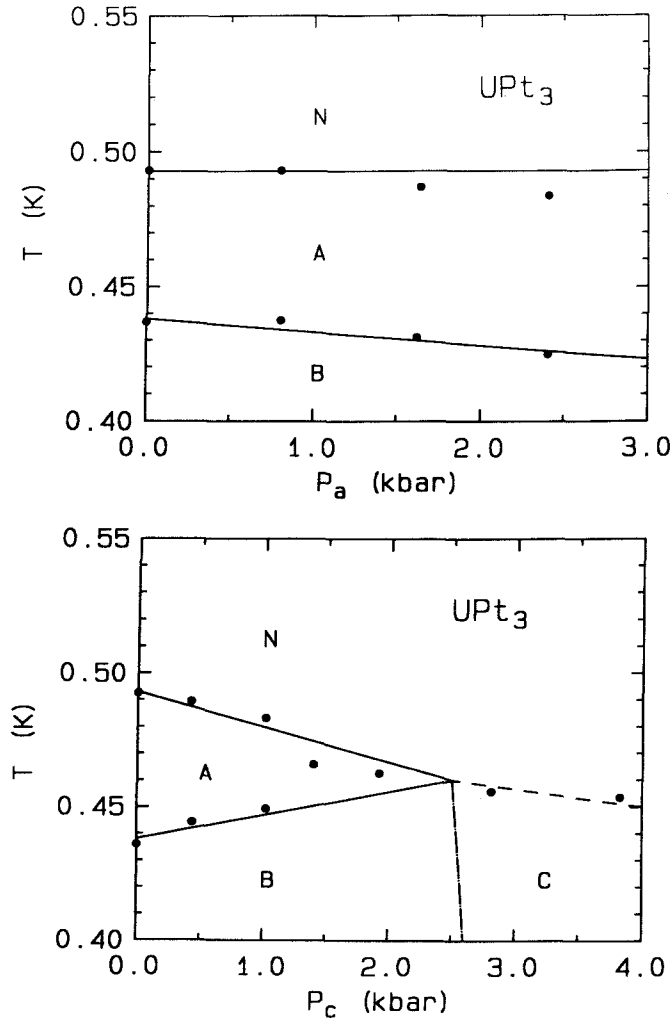

Fig. 8. Comparison of the calculated uniaxial pressure dependence of T_c according to eq. 3 and the measured values obtained by Jin *et al.*[26] (renormalised at T_c). The dashed dotted line represents the "missing" fourth phase line in the p_c-T plane.

TABLE III

Uniaxial (p_a and p_c) and Hydrostatic (p) Pressure Dependence of the Critical Temperatures T_c^+ and T_c^- of Superconducting UPt_3, Determined by Various Techniques.[21-26] The Hydrostatic Pressure Dependence is Given by $dT_c/dp = 2dT_c/dp_a + dT_c/dp_c$

	T_c^+	T_c^-	Method
dT/dp	−13(3)	—	ρ[21]
dT/dp	−24(5)	—	ρ[22]
dT/dp_a	0(1)	—	
dT/dp_c	−26(3)	—	onset χ_{AC}[23]
dT/dp	−26(3)	—	
dT/dp	−16(3)	—	onset c/T[24]
dT/dp	−24(5)	−5(1)	c/T[25]
dT/dp_a	−4(4)	−5(3)	
dT/dp_c	−13(3)	9(3)	c/T[20]
dT/dp	−21(6)	−1(5)	
dT/dp	−16(4)	0(4)	Ehrenfest[26]
dT/dp	−20(3)	0(3)	Ehrenfest[7]
dT/dp_a	0(2)	−5(2)	
dT/dp_c	−14(2)	9(2)	Ehrenfest
dT/dp	−14(3)	−1(3)	(this work)

The stability of the superconducting phases depends on the ratio β_2/β_1. A double superconducting transition is only found for $\beta_2/\beta_1 > \delta/\alpha_o T_{co} > 0$, for finite δ. In the absence of a *SBF* ($p_c > p_{cr}$) the model predicts the *B* phase to be stable for $\beta_2/\beta_1 > 0$, whereas a mixed state of the *A* and *C* phase is found for $-1 < \beta_2/\beta_1 < 0$. The experimental ratio β_2/β_1 has been determined from the steps in the specific heat at the *AB* and *NC* phase boundaries: $\beta_2/\beta_1 = (T_c^+/T_c^-)(\Delta c_{AB}/\Delta c_{NA})$. At zero pressure[4,7] β_2/β_1 amounts to 0.4, while under pressure (for $p_c \to p_{cr}$) β_2/β_1 increases slightly.[20,25] Therefore, the model calculation predicts the *B* phase to be stable under pressure in absence of a *SBF*. This is in clear contrast with the p_c-T phase diagram calculated from the Ehrenfest relations, where the *C* phase is the stable phase under pressure (for $p_c > p_{cr}$), as indicated in Fig. 8. The Ginzburg-Landau approach with a one-dimensional representation[13] leads to the same conclusions.

Therefore, it is of interest to investigate the constraints on the proposed Ginzburg-Landau models for a stable *C* phase in absence of a *SBF*. In order to get a reliable model prediction for the stability of the phase under pressure ($p_c > p_{cr}$) one should take into account the coupling of the order parameter to the internal strains.[28] For a coupling to the longitudinal strains the model parameters are modified by $\beta_1' = \beta_1 + G_{\gamma 1}(\varepsilon_{xx} + \varepsilon_{yy}) + G_{\gamma 1}'\varepsilon_{zz}$,

$\beta_2' = \beta_2 + G_{V2}(\varepsilon_{xx} + \varepsilon_{yy}) + G'_{V2}\varepsilon_{zz}$ and $T'_{co} = T_{co} - g_V(\varepsilon_{xx} + \varepsilon_{yy}) - g'_V\varepsilon_{zz}$. For a uniaxial pressure along the c-axis the longitudinal strains are described by $\varepsilon_{xx} = \varepsilon_{yy} = -s_{13}p_c$ and $\varepsilon_{zz} = -s_{33}p_c$, with compliances s_{13} and s_{33}. In the proposed Ginzburg-Landau scenario, where a nonzero ΔT_c results from a *SBF* for pressures below p_{cr}, the C phase can only be stable for pressures there above when $-1 < \beta_2'/\beta_1' < 0$. This may be achieved by a spontanuous change in the fourth order coupling constants G_{V2} and G'_{V2} at $p_c = p_{cr}$. In that case the A and C phase are mixed for $p_c > p_{cr}$, as they are degenerate in the absence of a *SBF*. This is a stringent condition as the ratio β_2'/β_1' should be positive for $p_c < p_{cr}$ in order to cause the splitting of T_c.

It is clear that the experimental results, in particular the pressure dependence of the phase diagram, impose severe constraints on the *SBF* scenario. These constraints urge to study in more detail alternative models, like the model of two nearly-degenerate order parameters of different representations.[29] Also the influence of the recently reported incommensurate structural modulation in the basal plane[30] is still unclear and needs further investigation.

6. CONCLUSIONS

The superconducting phase diagram of UPt_3 has been investigated by means of thermal-expansion and magnetostriction measurements. For all principal directions of the magnetic field ($B \| a$, $B \| b$ and $B \| c$) three different superconducting phases were found, meeting in a tetracritical point. The thermodynamic stability of the phase diagrams has been established. The four phase lines are likely of second order, although a weakly first order BC transition cannot be excluded. The pressure dependence of the phase diagrams was analysed using Ehrenfest relations. Also in the p_c-T plane a tetracritical point is found at $T_{cr} \simeq 0.460$ K and $p_{cr} \simeq 2.5$ kbar (using a linear extrapolation) for all field orientations. The C phase is found to be the most stable phase under pressure. This implies stringent constraints on the fourth order coupling constants in the Ginzburg-Landau scenario with a SBF. A direct measurement of the BC phase line under pressure would be highly desirable in order to elucidate this point.

ACKNOWLEDGMENTS

This work was part of the research program of the "Stichting FOM" (Foundation for Fundamental Research of Matter). The work of one of us (AdV) was made possible by a fellowship of the "KNAW" (Royal Netherlands Academy of Arts and Sciences).

REFERENCES

1. A. Sulpice, P. Gandit, J. Chaussy, J. Flouquet, D. Jaccard, P. Lejay, and J. L. Tholence, *J. Low Temp. Phys.* **62**, 39 (1986).
2. R. A. Fisher, S. Kim, B. F. Woodfield, N. E. Phillips, L. Taillefer, K. Hasselbach, J. Flouquet, A. L. Giorgi, and J. L. Smith, *Phys. Rev. Lett.* **62**, 1411 (1989).
3. T. Vorenkamp, Z. Tarnawski, H. P. van der Meulen, K. Kadowaki, V. J. M. Meulenbroek, A. A. Menovsky, and J. J. M. Franse, *Physica B* **163**, 564 (1990).
4. K. Hasselbach, L. Taillefer, and J. Flouquet, *Phys. Rev. Lett.* **63**, 93 (1989).
5. G. Bruls, D. Weber, B. Wolf, P. Thalmeier, B. Lüthi, A. de Visser, and A. Menovsky, *Phys. Rev. Lett.* **65**, 2294 (1990).
6. S. Adenwalla, S. W. Lin, Q. Z. Ran, Z. Zhao, J. B. Ketterson, J. A. Sauls, L. Taillefer, D. G. Hinks, M. Levy, and B. K. Sarma, *Phys. Rev. Lett.* **65**, 2298 (1990).
7. K. Hasselbach, A. Lacerda, K. Behnia, L. Taillefer, J. Flouquet, and A. de Visser, *J. Low. Temp. Phys.* **81**, 299 (1990).
8. R. Joynt, *Superc. Sci. Technol.* **1**, 210 (1988).
9. K. Machida, M. Ozaki, and T. Ohmi, *J. Phys. Soc. Jpn.* **58**, 4116 (1989).
10. R. Joynt, V. P. Mineev, G. E. Volovik, and M. E. Zhitomirsky, *Phys. Rev. B* **42**, 2014 (1990).
11. D. W. Hess, T. Tokuyasu, and J. A. Sauls, *J. Phys.: Cond. Mat.* **1**, 8135 (1989).
12. E. I. Blount, C. M. Varma, and G. Aeppli, *Phys. Rev. Lett.* **64**, 3074 (1990).
13. K. Machida, and M. Ozaki, *Phys. Rev. Lett.* **66**, 3293 (1991).
14. G. Aeppli, E. Bucher, C. Broholm, J. K. Kjems, J. Baumann, and J. Hufnagl, *Phys. Rev. Lett.* **60**, 615 (1988).
15. R. Joynt, *J. Magn. Magn. Mat.* **108**, 31 (1992).
16. S. K. Yip, T. Li, and P. Kumar, *Phys. Rev. B* **43**, 2742 (1991).
17. N. H. van Dijk, A. de Visser, J. J. M. Franse, S. Holtmeier, L. Taillefer, and J. Flouquet, *Phys. Rev. B* **48**, 1299 (1993).
18. B. Bogenberger, H. von Löhneysen, T. Trappmann, and L. Taillefer, *Physica B* **186–188**, 248 (1993).
19. S. Adenwalla, J. B. Ketterson, S. K. Yip, S. W. Lin, M. Levy, and B. K. Sarma, *Phys. Rev. B* **46**, 9070 (1992).
20. D. S. Jin, S. A. Carter, B. Ellman, T. F. Rosenbaum, and D. G. Hinks, *Phys. Rev. Lett.* **68**, 1597 (1992).
21. J. O. Willis, J. D. Thompson, Z. Fisk, A. de Visser, J. J. M. Franse and A. Menovsky, *Phys. Rev. B* **31**, 1654 (1985).
22. K. Behnia, L. Taillefer, and J. Flouquet, *J. Appl. Phys.* **67**, 5200 (1990).
23. M. Greiter, C. G. Lonzarich, and L. Taillefer, *Phys. Lett. A* **169**, 199 (1992).
24. G. E. Brodale, R. A. Fisher, N. E. Phillips, G. R. Stewart, and A. L. Giorgi, *Phys. Rev. Lett.* **57**, 234 (1986).
25. H. von Löhneysen, T. Trappmann, and L. Taillefer, *Phys. Rev. B* **43**, 13714 (1991).
26. A. de Visser, A. A. Menovsky, J. J. M. Franse, K. Hasselbach, A. Lacerda, L. Taillefer, P. Haen, and J. Flouquet, *Phys. Rev. B* **41**, 7304 (1990).
27. S. M. Hayden, L. Taillefer, C. Vettier, and J. Flouquet, *Phys. Rev. B* **46**, 8675 (1992).
28. P. Thalmeier, B. Wolf, D. Weber, G. Bruls, B. Lüthi, and A. A. Menovsky, *Physica C* **175**, 61 (1991).
29. I. Luk'yanchuk, *J. Phys. I* **1**, 1155 (1991).
30. P. A. Midgley, S. M. Hayden, L. Taillefer, B. Bogenberger, and H. von Löhneysen, *Phys. Rev. Lett.* **70**, 678 (1993).